GRID FEED-IN BEHAVIOR OF DISTRIBUTED PV BATTERY SYSTEMS

Johannes Weniger, Joseph Bergner, David Beier, Marc Jakobi, Tjarko Tjaden, Volker Quaschning
HTW Berlin - University of Applied Sciences
Wilhelminenhofstraße 75A, 12459 Berlin, Germany
http://pvspeicher.htw-berlin.de

ABSTRACT: This paper analyzes the cumulative grid feed-in behavior of distributed PV battery systems. Simulations with a time resolution of 1 s were performed to determine the impact of the feed-in limit and respective moving average interval on the power flows fed into the grid by spatially dispersed PV battery systems. The study focuses on the main question: What is the impact of different averaging intervals on the grid feed-in behavior of a distributed fleet of PV battery systems? The simulation results reveal that the peaks in the overall feed-in power can be mitigated by reducing the averaging interval from 10 min to 1 min or less.
Keywords: PV Battery Systems, Battery Storage, Grid Integration, Feed-in Limitation, Peak Shaving

1 INTRODUCTION

Considering the increasing amount of PV electricity produced in Germany, new challenges with regard to the grid integration of PV systems are coming up. Especially distribution grids with a high PV penetration are affected by voltage rises and reverse power flows induced by PV peak injection around noon [1]. To tackle these challenges, several solutions have been developed and implemented in the regulatory framework in recent years. With the revision of the German Renewable Energy Act (EEG) in 2012, a feed-in power limitation to 70% of the installed PV power (0.7 kW/kWp) was introduced for PV systems with a rated power less than 30 kWp alternatively to the participation in the grid operator´s feed-in management (Figure 1).

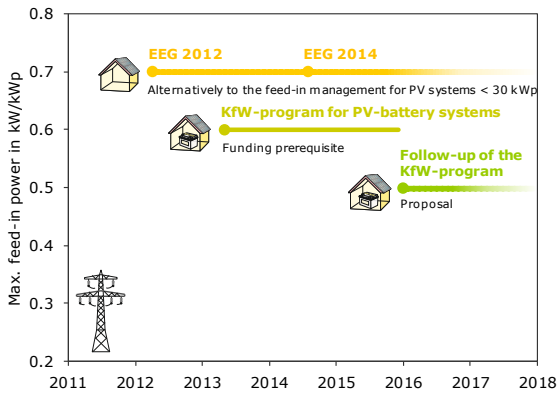

Figure 1: Implementation of incentives in the German regulatory framework to limit the feed-in power of PV systems and PV battery systems.

Apart from the EEG, a market incentive program for small-scale battery systems was established by the German government-owned development bank KfW in May 2013. To obtain the repayment grants and loans with reduced interest rates of the funding scheme, the feed-in power of the subsidized PV battery systems has to be restricted to 0.6 kW/kWp. Currently, the continuation of the incentive program from the beginning of 2016 onwards with a reduced feed-in limit of 0.5 kW/kWp is under discussion.

In principal, the feed-in limit incentivized by the funding program aims to shift the battery charging to times of high PV production and thereby to reduce feed-in peaks. Nevertheless, most commercially available PV battery systems operate in a way that charges the battery as soon as excess PV power is available [2]. In consequence, the battery frequently reaches its maximum state of charge before noon, especially on clear days. To maintain the funding prerequisite, surplus PV power that exceeds the feed-in limit has to be curtailed. Hence, feed-in peaks are often not shaved by charging the battery, but by throttling the PV power output. To prevent the PV system operator from these unnecessary curtailment losses while maintaining a high energy throughput of the battery system, the battery charging has to be scheduled based on forecasts of the PV generation and load consumption [3]. In this way, PV energy that exceeds the permitted feed-in limit can be used to charge the battery system, which reduces the amount of PV energy that has to be curtailed.

Furthermore it is defined that the feed-in limitation refers to the mean value of the grid injection over a period of 10 min [4]; i.e. as long as the moving 10 min average of the feed-in power does not exceed the limit, short-term feed-in peaks for several seconds or minutes are permitted. So far most studies that have investigated the impact of PV battery systems on distribution grids don’t take this aspect into account and simulate the grid feed-in behavior with a temporal resolution of 1 min or larger [5]–[8]. Hence, this paper focuses on the question: Is the moving averaging interval of 10 min appropriate to reduce the grid feed-in peaks of a distributed fleet of PV battery systems?

The paper is organized as follows. In the next section the grid injection of a single PV battery system is investigated with a temporal resolution of 1 s over a whole year. Section 3 presents the feed-in behavior of a variety of spatially dispersed PV battery systems for one exemplary day; followed by a load flow simulation of a distribution grid in section 4. The findings are discussed in section 5. Finally, section 6 concludes this paper.

2 GRID FEED-IN POWER OF ONE SINGLE PV BATTERY SYSTEM

In this section, the grid feed-in behavior of a household equipped with a PV battery system is analyzed. The first subsection describes the used input data, simulation models and control schemes. In the second subsection, the simulation results are presented and assessed from an energetic point of view.

2.1 Methodology

In this investigation the power output of the PV system is simulated based on meteorological measurements from the University of Oldenburg [9]. The dataset includes measured values of the air temperature, diffuse and global irradiance with a temporal resolution of 1 s from the year 2014. The measurements are used to calculate the irradiance for each second on a south oriented und 35° declined PV generator. A detailed description of the applied models to simulate the PV power output can be found in [10]. The PV output is scaled to a rated PV power of 10 kWp. Additionally, the apparent power of the inverter is set to 1 kVA/kWp and the reactive power provision is taken into account with a fixed power factor of 0.95, thus limiting the active power to 0.95 kW/kWp.

A further data basis is provided by two measured datasets with time series of the electricity consumption of various households. Measurements from the Institute for Future Energy Systems (IZES) and Vienna University of Technology (TU Wien) have been used to synthesize several load profiles with a 1 s resolution for a whole year [11]. The following investigation is based on the load profile of a household with an annual load demand of 5 MWh.

The PV power output and the electrical load are used to determine the excess PV power that can be used to charge the battery system. In this paper, the AC-coupled battery system based on a lithium-ion battery has been modeled by constant efficiency factors [10]. The usable battery capacity is assumed to be 10 kWh. The battery system is operated conventionally by charging it with the first available PV surpluses in the morning.

According to the current requirements of the KfW´s market incentive program, the grid feed-in limitation is set to 0.6 kW/kWp. A corresponding averaging interval of 10 min serves as a reference, which is named “10 min limitation” in the following. It is necessary to distinguish between the more illustrative averaging interval for the plots and the controller relevant limitation interval.

Several control strategies are applicable to avoid the exceedance of the predefined limit with regard to the corresponding moving average of the feed-in power. To ensure comparability between different limitation intervals, a straightforward approach is implemented in the control unit. The actual grid feed-in power is directly limited to guarantee the adherence of the limit over the preceding averaging interval without using sophisticated control loop feedback mechanisms.

2.2 Simulation Results

Based on the described input data and system models, the energy flows of a household equipped with a PV battery system are simulated over a period of 1 year with 1 s resolution. The usage of the produced PV power during a day with a clear sky in the morning and partly cloudy conditions in the afternoon is shown in Figure 2. For better visibility, the energy flows are plotted as 10 min moving averages. The PV power output used directly by the load is depicted by the yellow area. The excess PV power is primarily used for charging the battery, colored in green. As long as the 10 min average of the resulting surpluses does not exceed the defined feed-in limit, the entire surplus PV power is fed into the grid. However, it can be observed that curtailing of PV power around noon is required to prevent the 10 min moving average of the feed-in from exceeding the limit.

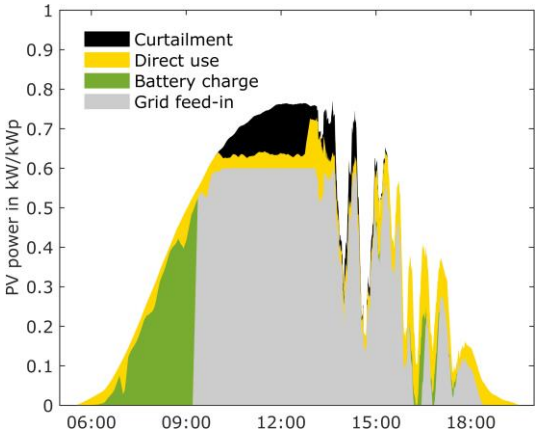

Figure 2: Energy flows of a PV battery system during an exemplary day in a temporal resolution of 10 min (feed-in limit 0.6 kW/kWp, limitation interval 10 min).

Whereas the 10 min average values do not exceed the feed-in limit, the values with a resolution of 1 s exceed the threshold significantly, as shown in Figure 3. Without any feed-in limitation, fluctuations in the excess PV power are already caused by passing clouds as well as by load spikes due to switching electrical devices. Additionally, the control scheme maintaining the feed-in limitation causes high fluctuations in the feed-in power. This is due to the fact that a feed-in peak above the limit can be compensated by a preceding drop in the PV power without exceeding the threshold. Conversely, an excessive grid injection period has to be leveled out by a subsequent feed-in power reduction realized by PV curtailment. This oscillating curtailment of PV power can enhance the fluctuations in the grid feed-in power.

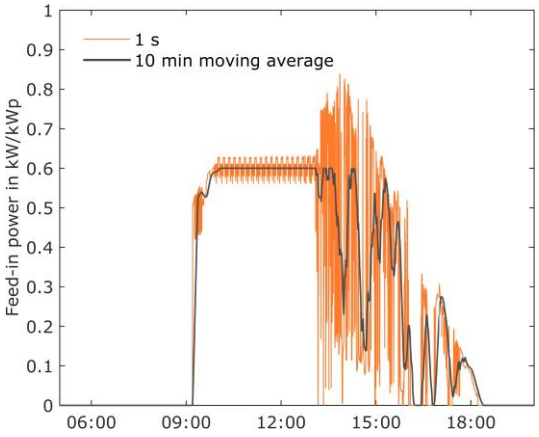

Figure 3: Feed-in power of a PV battery system during an exemplary day in different temporal resolution (feed-in limit 0.6 kW/kWp, limitation interval 10 min).

In order to gain a better understanding of the resulting feed-in peaks, Figure 4 compares the grid injection of different averaging intervals during a period with fluctuating PV output. The curve of the excess PV power without any limitation reveals that surpluses above the feed-in limit occur. All other curves keep the maximum feed-in limit of 0.6 kW/kWp within the

particular interval. For the reference case with a 10 min average feed-in limitation an active adjustment of the feed-in power is required towards the end of the chosen period. During the adjustment, the feed-in power values are similar to the values 10 min before. Consequently, steep slopes of the grid feed-in occur and grid injection patterns are repeated. Reducing the averaging interval to 1 min results in a feed-in pattern which is repeated every minute. Therefore, the intermittent appearance of the grid feed-in is increased. Moreover, it can be seen that a feed-in limitation each second creates no additional fluctuations and avoids short-term peaks above the feed-in limit as well.

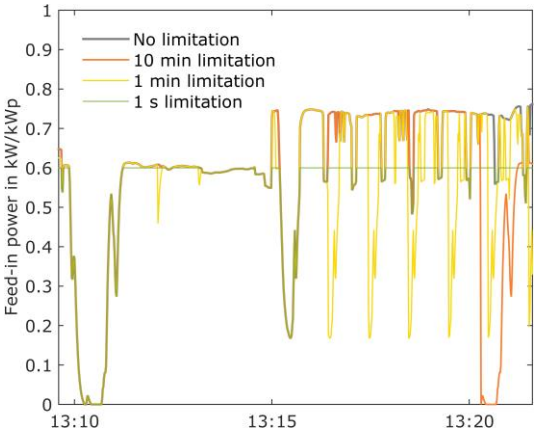

Figure 4: Feed-in power of a PV battery with different limitation intervals in 1 s time resolution during a period with fluctuating PV output (feed-in limit 0.6 kW/kWp).

Distinctions in the feed-in power of the investigated system with different limitation intervals applied can also be found in the annual simulation results, shown in Figure 5. The presented annual duration curves are obtained by sorting the calculated values of the feed-in power over the period of one year. It is clearly visible that the 10 min as well as 1 min feed-in limitation cannot prevent the grid injection from exceeding the threshold value. In both cases, the resulting maximum feed-in power does not differ from the maximum of the system without a feed-in limitation. Nevertheless, a reduction of the respective averaging interval from 10 min to 1 min lowers the dwell time at high feed-in power levels. As already stated above, the simulated 1 s feed-in limitation allows the adherence of the threshold at any time of the year. As a consequence, the exceedance of the feed-in limit in short time scales can in theory only be avoided by an instantaneous feed-in limitation.

Whereas the grid operator is usually interested in restricting the maximum PV feed-in power for grid dimensioning reasons, the system owner aims to minimize the energy losses due to curtailment and thus to maximize the energy exported to the grid. Table I quantifies the annual curtailment losses for the PV battery system with the above mentioned specifications. The curtailment losses are calculated for varying feed-in limits and limitation intervals. In general, it can be seen that with a decreasing feed-in limit the curtailed PV energy is increased.

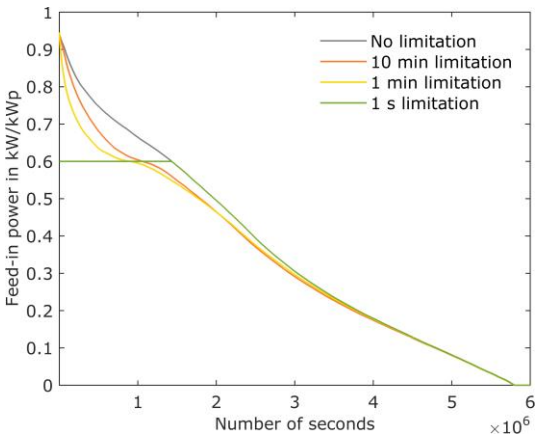

Figure 5: Annual duration curves of the feed-in power of a PV battery system with different limitation intervals in 1 s time resolution (feed-in limit 0.6 kW/kWp).

In the reference case about 3.7% of the possible annual PV energy output has to be curtailed for the specific system configuration. The reduction of the limitation interval from 10 min to 1 min results in curtailment losses of 4.7%. Hence, the shorter the average interval, the larger the curtailment losses will be. Considering these facts, larger limitation intervals and higher feed-in limits are beneficial for the system owner, as more PV energy can be fed into the grid. In summary, it could be seen that a compromise with regard to the length of the limitation interval is required.

Table I: Annual curtailment losses as a function of the feed-in limit and limitation interval for a PV battery system that charges the battery as soon as possible (PV system size 10 kWp, usable battery capacity 10 kWh).

Feed-in limit in kW/kWp	0.7	0.6	0.5	0.4
1 s	1.9%	5.0%	9.7%	15.9%
1 min	1.7%	4.7%	9.5%	15.7%
10 min	1.1%	3.7%	8.2%	14.4%

3 GRID FEED-IN POWER OF DISTRIBUTED PV BATTERY SYSTEMS

The preceding section focuses on grid injection peaks of a single PV battery system. In the following, it is analyzed how short-term fluctuations of the grid feed-in affect the cumulative feed-in behavior of spatially dispersed PV battery systems on an exemplary day.

3.1 Methodology

The number of households equipped with a PV battery system and their spatial disposition was chosen with regard to the typical village grid as presented in [12]. The village grid connects 57 households and consists of 6 feeders each with 4 to 16 points of common coupling (see Figure 6). The feeders are aligned in a radial fashion with different orientations. A household with a PV battery system was assigned to each point of common coupling.

The PV power output was modeled based on the aforementioned dataset for a day with high fluctuations in

the irradiance profile caused by passing clouds. In order to take temporal and spatial discrepancies in the PV power output into account, an individual PV generation profile was created for each PV system with regard to their geographic position. This was realized by delaying the irradiance profile from the western to the eastern PV systems. Orthogonal to the wind direction a homogenous cloud cover is assumed. The cloud velocity is typically in the range of 10 to 20 m/s [13] and is assumed to be 10 m/s in this study. As the maximum east-west extent between two PV systems is about 850 m, the maximum time lag between two PV generation profiles is 85 s.

An individual daily load profile with a temporal resolution of 1 s was assigned to each household based on a dataset of the TU Wien [14]. The measurements include both active and reactive power consumption of the households. The PV systems and battery storages are modeled according to section 2.1. Hence, all households have an identically rated PV power of 10 kWp and a usable battery capacity of 10 kWh.

3.2 Simulation Results

In the following, the temporal and spatial differences in the grid injection of the 57 PV battery systems with a total PV capacity of 570 kWp are analyzed. Figure 6 compares the calculated site-specific feed-in power at two simulation time steps. Differences in the feed-in power of the distributed PV battery systems are attributable among other things to the spatially varying global irradiance conditions as well as individual load profiles of the households.

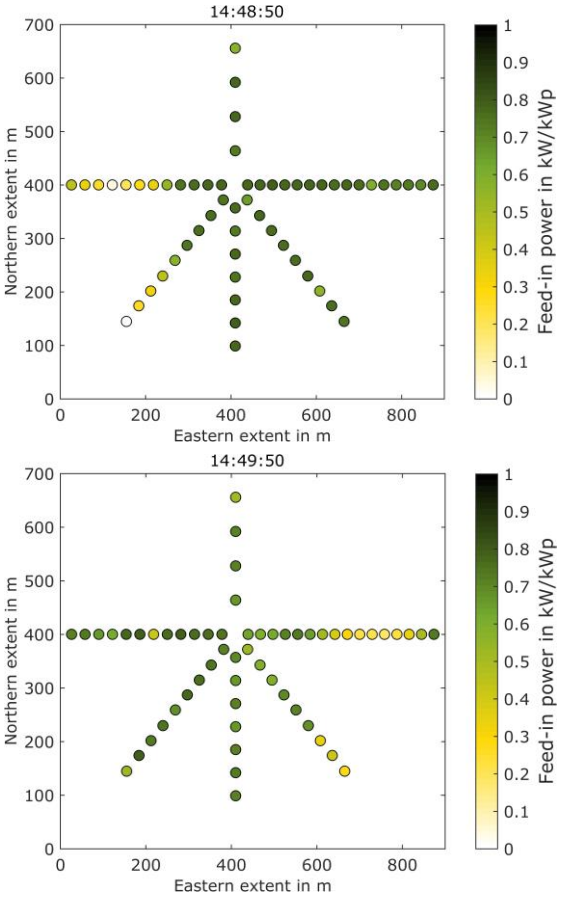

Figure 6: Feed-in power of 57 PV battery systems at two instants of time over a period of 1 min.

At the first instant of time a drop in the grid injection due to cloudy conditions can be observed in the western feeder whereas the other systems feed at high power levels into the grid (Figure 6 top). About 60 s later, the reduced feed-in power levels occur in the eastern feeder because of the shift in the PV generation profile and assumed wind direction (Figure 6 bottom). By comparing both graphs, a high spatial and temporal variability of the grid injection is visible during periods of fluctuating cloud cover.

Figure 7 shows the cumulative feed-in power of the 57 PV battery systems during the exemplary day for different limitation intervals. Despite the spatial extent of the investigated fleet, the grid injection without any limitation shows a strongly fluctuating characteristic. The fluctuations are increased further by the control approach reacting on the 10 min limitation interval. Hence, for the investigated arrangement of the PV battery systems the averaging interval of 10 min is not sufficient to mitigate the total feed-in power due to spatial smoothing not occurring at all. Compared to the energy flows of the single system (see Figure 4), it is apparent that the overall grid injection is smoothed by applying a 1 min limitation interval. However, short-term feed-in peaks lasting several seconds still exceed the feed-in limit. These peaks are only avoided by the instantaneous feed-in limitation. These findings reveal the importance of highly temporally resolved simulations to render the variability of the feed-in power visible.

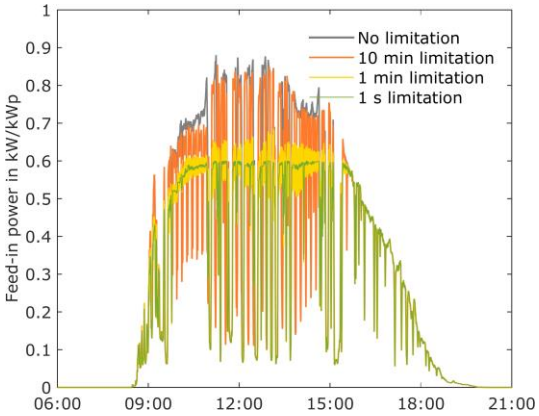

Figure 7: Cumulative feed-in profile of 57 PV battery systems with different limitation intervals depicted as 1 s instantaneous values.

4 GRID SIMULATION

After solely observing the spatial and temporal variability of the grid feed-in power in the previous sections, the following will analyze the voltage situation of a distribution grid equipped with the 57 PV battery systems for different limitation intervals. The investigation is based on the calculated energy flows of the exemplary day presented in section 3.

4.1 Methodology

The grid simulation was modeled as a steady-state power flow problem and solved with the Newton-Raphson algorithm using Matpower [15]. The model was used to perform a time series simulation with an increment of 1 s for the chosen low voltage grid. The

electrical parameters were set following the empirically derived and representative low voltage grids in [12]. In particular, the investigated village grid consists of 6 feeders with a length ranging from 256 to 464 m and a total number of connected households of 57. The geographical extension of the network has already been depicted in Figure 6. Table II shows the assumed electrical parameters of the modeled grid components. The cables were only modeled right to the point of common coupling.

Table II: Impedance of the modeled electrical equipment of the investigated distribution grid.

Electrical equipment	Impedance in Ω/km
Cable type NAYY 4x150 mm²	0.208 + j 0.008
10 / 0.4 kV Transformer S=400 kVA	0.0046 + j 0.015

The normalized voltage has been set to the allowed maximum of 106% at the medium voltage level as this constitutes the worst case for the voltage stability in low voltage grids [12], [17]. Depending on the ratio of inductive reactive power to active power, the voltage at the transformer's low voltage side can be lower due to the transformers relatively high reactance.

In Germany the technical regulation VDE-AR-N 4105 states that the voltage increase caused by decentralized grid feed-in must not exceed 3% of the nominal voltage in every point of common coupling in the grid in a 10 min interval [16]. Additionally, the DIN EN 50160 defines that the 10 min average values have to stay below +10% of the nominal voltage [17]. Therefore, this can be considered as a defined limit for the PV penetration in low voltage grids. Hence, the following section will analyze the influence of the moving averaging interval on the voltage increase.

4.2 Simulation Results

Figure 8 shows the voltage at each point of common coupling in the grid as a function of the distance from the local power transformer for the two instants of time investigated in Figure 6. As the overall impedance and the power injection increase with the length of the feeder, the points of common coupling at the end of the east- and the west-orientated feeders would be typically most critical for voltage rises under clear sky conditions.

At the first instant of time the maximum voltage can be found at the end of the eastern feeder, as a cloud affects the feed-in power in the western part of the grid (see Figure 6). About 60 s later, decreased voltages in the eastern feeder and voltage peaks in the western part are visible. As a result, the voltage maximum switches from the end of the eastern feeder to the end of the western feeder. The comparison of these two time steps reveals the short-term fluctuations in the voltage level across the grid. In general, the short-term dynamic accelerates in situations with faster cloud motion or with cloud directions orthogonally towards a feeder. In these cases, steep voltage ramps can be seen in the feeders.

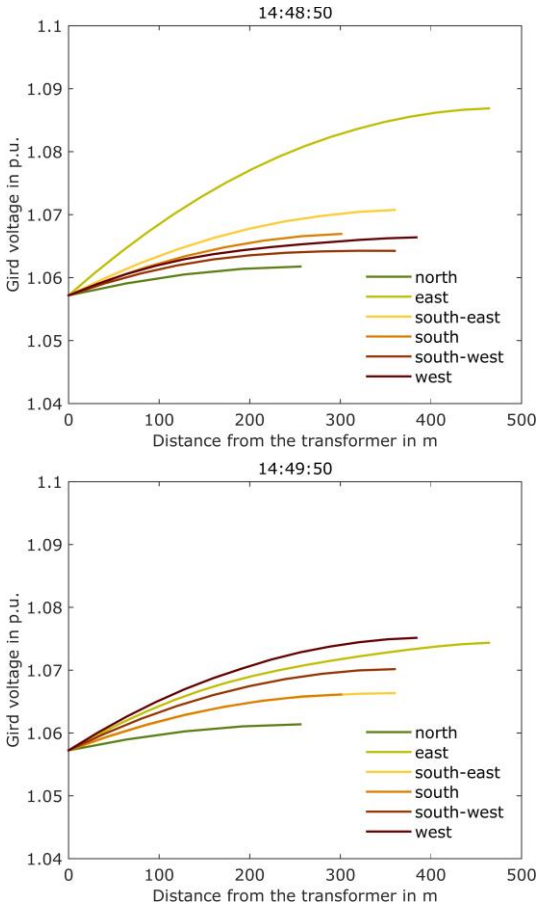

Figure 8: Grid voltage as function of the distance from the substation for the six feeders at two instants of time.

Figure 9 analyzes the maximum voltage in the grid for different averaging intervals of the feed-in limitation. The maximum voltage was determined by extracting the highest voltage occurring in the grid for each time step. The top graph shows a good correlation to the resulting power flows presented in section 3. It becomes apparent that a 10 min averaging interval for the controller cannot reduce peak voltages, even though there might be balancing effects caused by the passing clouds or different load consumption. Despite the feed-in-limit being applied, the maximum voltage in the grid cannot be reduced substantially. The resulting voltages from the 1 min limitation interval show a similar dynamic. The instantaneous feed-in power control leads to significantly reduced fluctuations in the maximum voltage. In contrast to the control approach using a moving averaging interval as a benchmark the changes in peak voltages in the grid are almost completely induced by the cloud movement as well as the consumed load while controller induced fluctuations are eliminated.

The bottom graph also depicts the maximum voltage for the different limitation intervals but in contrast to the top one the 10 min moving average values for each curve are plotted. Therefore, it shows a much smoother shape. Without any feed-in limitation also the 10 min averaged values of the maximum grid voltage exceeds the 1.09 p.u. threshold. For all limitation intervals, the voltage peaks are reduced significantly in a 10 min time resolution. Nevertheless, only small differences between the distinct limitation intervals can be observed.

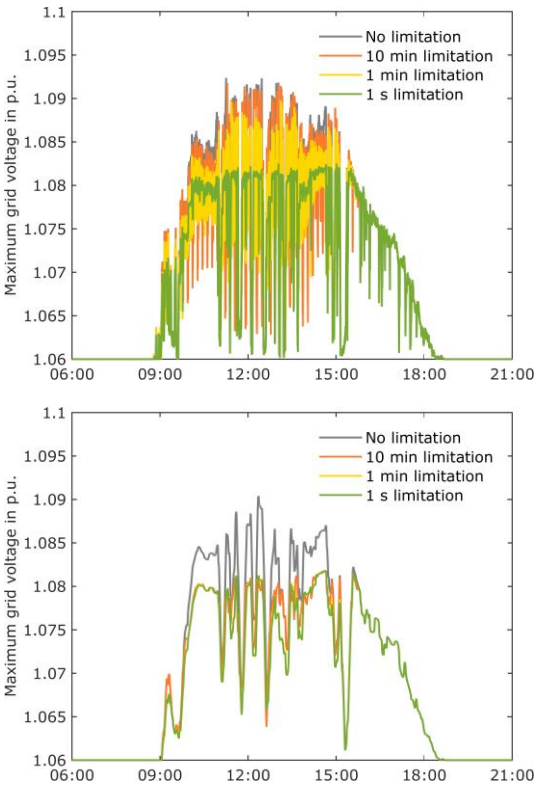

Figure 9: Maximum grid voltage of all points of common coupling for different limitation intervals in 1 s (top) and 10 min time resolution (bottom).

5 DISCUSSION

In this section, the simulation results and findings should be discussed. First, it needs to be mentioned that the simulation setting and the investigation are of a theoretical nature. Every household in the investigated grid was equipped with a PV battery system which corresponds to a very high penetration. Uniform orientations and specifications have been assumed for all PV systems, which leads to a high simultaneity in the PV generation. Furthermore, the spatial and temporal differences in the PV power output have been modeled with a simple approach. One site-specific measured irradiance profile was assigned to several sites taking a delay with regard to the geographical position as well as the assumed wind direction and velocity into account. Every site orthogonal to the wind direction was assigned with the same irradiance value thus neglecting spatial differences in the cloud cover. By considering this aspect, the spatial differences in the PV output might be higher in practice. On the other hand, a higher cloud velocity could reduce the spatial balancing between the PV system sites. Furthermore, the spatial smoothing is also highly sensitive to the layout of the investigated distribution grid. Hence, further investigations are needed to identify whether the findings are also applicable for other distribution grids.

Apart from the simulation setting, the results are also affected by the used control scheme of the feed-in limitation. The current feed-in power was adjusted to avoid that the respective moving average exceeds the feed-in limit. This control approach is beneficial for the system owner due to low curtailment losses. Nevertheless, such a control scheme can enhance the fluctuations in the grid injection and grid voltage. Hence, the electrical facilities would be stressed with more alternating power in addition to the cloud-induced variability which may lead to reduced lifetime expectancies. Apart from the network operating equipment, the domestic appliances are also affected from fluctuations and peaks in the grid voltage, which may reduce the device lifetime.

The simulation results with varying limitation intervals reveal that averaging intervals shorter than 10 min might be useful to mitigate short-term feed-in peaks. Hence, a revision of the current regulatory framework by establishing shorter limitation intervals can improve the grid integration of PV battery systems further. Nevertheless, by defining a moving average of the feed-in power as the benchmark uncertainties regarding the parameterization of the controllers realizing the feed-in limitation remain. From the grid perspective, an instantaneous feed-in limitation would be the optimal solution. Nevertheless, due to the inherent response time of PV battery systems an instantaneous feed-in limitation is very difficult to put into practice.

6 CONCLUSIONS

In this paper, the impact of various limitation intervals on the grid injection have been studied for a single PV battery system and a spatially dispersed fleet of PV battery systems. The simulation results reveal that short-term feed-in peaks above the feed-in limit cannot be avoided by limiting the grid injection to their average value over the preceding 10 min. Due to the high simultaneity in the feed-in power of the investigated fleet of PV battery systems, a conventional 10 min limitation is not sufficient to guarantee a balancing between the systems for reasons of spatial smoothing effects.

By applying a 1 min feed-in limitation instead of a 10 min limitation, the magnitude of the short-term feed-in peaks is mitigated. However, to prevent the feed-in power from exceeding the limit at each instant of time, an instantaneous feed-in limitation is required. Shorter limitation intervals result in higher curtailment losses, which are adverse for the system owner, though. By comparing the simulation results with different limitation intervals it can be supposed that an adjustment in the regulatory framework towards lower averaging intervals can improve the grid integration of PV battery systems further.

ACKNOWLEDGEMENT

The authors thank the German Federal Ministry of Economics and Technology (BMWi) and the Projektträger Jülich (PtJ) for the support of the project “LAURA/PVstore” (grant agreement no. 0325716G). Furthermore, the authors thank the University of Oldenburg and the Vienna University of Technology for the provision of measurements. The authors are solely responsible for the content of this publication.

REFERENCES

[1] G. Wirth, A. Spring, G. Becker, R. Pardatscher, R. Witzmann, J. Brantl, and M. Garhamer, "Effects of a high PV Penetration on the Distribution Grid," in *27th European Photovoltaic Solar Energy Conference and Exhibition*, Frankfurt am Main, 2012, pp. 3740–3744.

[2] M. Fuhs, "Marktübersicht Batteriespeicher," *pv magazine*, pp. 28–39, Jun-2015.

[3] J. Weniger, J. Bergner, and V. Quaschning, "Integration of PV power and load forecasts into the operation of residential PV battery systems," in *4th Solar Integration Workshop*, Berlin, 2014.

[4] "Connecting and operating storage units in low voltage networks," Verband der Elektrotechnik Elektronik Informationstechnik e. V. (VDE), Berlin, Jun. 2013.

[5] J. Struth, M. Leuthold, A. Aretz, M. Bost, S. Gährs, M. Cramer, E. Szczechowicz, B. Hirschl, A. Schnettler, D. U. Sauer, and K.-P. Kairies, "PV-Benefit: A critical review of the effect of grid integrated pv-storage-systems," in *8th International Renewable Energy Storage Conference and Exhibition*, Berlin, 2013.

[6] J. von Appen, T. Stetz, M. Braun, and A. Schmiegel, "Local Voltage Control Strategies for PV Storage Systems in Distribution Grids," *IEEE Trans. Smart Grid*, vol. 5, no. 2, pp. 1002–1009, Mar. 2014.

[7] F. Marra, G. Yang, C. Traeholt, J. Ostergaard, and E. Larsen, "A Decentralized Storage Strategy for Residential Feeders With Photovoltaics," *IEEE Trans. Smart Grid*, vol. 5, no. 2, pp. 974–981, Mar. 2014.

[8] M. Resch, B. Ramadhani, J. Bühler, and A. Sumper, "Comparison of control strategies of residential PV storage systems," in *9th International Renewable Energy Storage Conference and Exhibition (IRES 2015)*, Düsseldorf, 2015.

[9] J. Kalisch, T. Schmidt, D. Heinemann, and E. Lorenz, "Continuous meteorological observations in high-resolution (1Hz) at University of Oldenburg in 2014." 10.1594/PANGAEA.847830, 2015.

[10] J. Weniger, T. Tjaden, and V. Quaschning, "Sizing of Residential PV Battery Systems," *Energy Procedia*, vol. 46, pp. 78–87, 2014.

[11] J. Weniger, J. Bergner, T. Tjaden, J. Kretzer, F. Schnorr, and V. Quaschning, "Einfluss verschiedener Betriebsstrategien auf die Netzeinspeisung räumlich verteilter PV-Speichersysteme," in *30. Symposium Photovoltaische Solarenergie*, Bad Staffelstein, 2015.

[12] G. Kerber, "Aufnahmefähigkeit von Niederspannungsverteilnetzen für die Einspeisung aus Photovoltaikkleinanlagen," Dissertation, Technische Universität München, München, 2011.

[13] J. Scheffler, "Bestimmung der maximal zulässigen Netzanschlussleistung photovoltaischer Energie-wandlungsanlagen in Wohnsiedlungsgebieten," Dissertation, Technische Universität Chemnitz, Chemnitz, 2002.

[14] A. Einfalt, A. Schuster, C. Leitinger, D. Tiefgraber, M. Litzlbauer, S. Ghaemi, D. Wertz, A. Frohner, and C. Karner, "Konzeptentwicklung für ADRES - Autonome Dezentrale Erneuerbare Energie Systeme," Wien, Endbericht, Aug. 2012.

[15] R. Zimmermann and C. Murillo-Sanchez, "MATPOWER: Steady-State Operations, Planning and Analysis Tools for Power Systems Research and Education," *IEEE Transactions on Energy Conversion*, vol. 1, no. 26, pp. 12–19, Feb-2011.

[16] VDE, "VDE-AR-N 4105: Erzeugungsanlagen am Niederspannungsnetz - Technische Mindest-anforderungen für Anschluss und Parallelbetrieb von Erzeugungsanlagen am Niederspannungs-netz." VDE-Verlag, 2011.

[17] DIN EN 50160-2008, "Merkmale der Spannung in öffentlichen Elektrizitätsversorgungsnetzen."